Published in final edited form as:
Neurology. 2002 March 26; 58(6): 928–935.

Selective reduction of *N*-acetylaspartate in medial temporal and parietal lobes in AD

N. Schuff, PhD, **A.A. Capizzano, MD**, **A.T. Du, MD**, **D.L. Amend, PhD**, **J. O'Neill, PhD**, **D. Norman, MD**, **J. Kramer, PhD**, **W. Jagust, MD**, **B. Miller, MD**, **O.M. Wolkowitz, MD**, **K. Yaffe, MD**, and **M.W. Weiner, MD**

From the Magnetic Resonance Unit (Drs. Schuff, Du, Amend, and Weiner), DVA Medical Center San Francisco; Departments of Radiology (Drs. Norman and Weiner), Neurology (Drs. Miller, Yaffe, and Weiner), Medicine (Dr. Weiner), and Psychiatry (Dr. Wolkowitz), University of California, San Francisco; MRI Unit (Dr. Capizzano), Fernández Hospital, Buenos Aires, Argentina; Department of Radiology (Dr. O'Neill), University of California, Los Angeles; and Department of Neurology (Dr. Jagust), University of California, Davis

Abstract

Background—Both AD and normal aging cause brain atrophy, limiting the ability of MRI to distinguish between AD and age-related brain tissue loss. MRS imaging (MRSI) measures the neuronal marker *N*-acetylaspartate (NAA), which could help assess brain change in AD and aging.

Objectives—To determine the effects of AD on concentrations of NAA, and choline- and creatine-containing compounds in different brain regions and to assess the extent NAA in combination with volume measurements by MRI improves discrimination between AD patients and cognitively normal subjects.

Methods—Fifty-six patients with AD (mean age: 75.6 ± 8.0 years) and 54 cognitively normal subjects (mean age: 74.3 ± 8.1 years) were studied using MRSI and MRI.

Results—NAA concentration was less in patients with AD compared with healthy subjects by 21% ($p < 0.0001$) in the medial temporal lobe and by 13% to 18% ($p < 0.003$) in parietal lobe gray matter (GM), but was not changed significantly in white matter and frontal lobe GM. In addition to lower NAA, AD patients had 29% smaller hippocampi and 11% less cortical GM than healthy subjects. Classification of AD and healthy subjects increased significantly from 89% accuracy using hippocampal volume alone to 95% accuracy using hippocampal volume and NAA together.

Conclusion—In addition to brain atrophy, NAA reductions occur in regions that are predominantly impacted by AD pathology.

Brain MRI in patients with AD shows substantial volume losses of the hippocampus[1] and cortical gray matter (cGM),[2,3] presumably reflecting AD-related deterioration of neuronal processes, neuron shrinkage, and neuron death. Cognitive normal (CN) elderly subjects also show volume losses in these regions, although to a lesser degree than AD[4,5], but this age-related volume decline may be related to a different mechanism than AD[6,7]. Furthermore, reactive gliosis after neuronal damage may attenuate volume loss. Therefore, the ability of MRI to distinguish between AD and normal aging based on brain atrophy is limited.

In vivo proton MRS (^{1}H MRS) measures *N*-acetylaspartate (NAA), which is present at high concentration only in living neurons and is virtually undetectable in other cell types, such as

Address correspondence and reprint requests to Dr. Norbert Schuff, DVA Medical Center, 4150 Clement St. 114M, San Francisco, CA 94121; e-mail: nschuff@itsa.ucsf.edu.

Supported in part by NIH grants AG10897 and AG12435 and a grant from the Alzheimer's Association.

glial cells.[8] Therefore, NAA is thought to be an indicator of neuronal density and neuronal metabolism.[9,10] ^{1}H MRSI also detects creatine (Cr, which reflects high-energy phosphate metabolism) and choline metabolites (Cho, which presumably reflect cellular membrane integrity). Several MRS studies found NAA reductions in AD relative to other metabolites[11,12] or reduced NAA concentrations (not referenced to other metabolites and corrected for tissue volume)[13–16] compared with normal aging. However, most previous studies used single voxel MRS localization techniques, thus information about the regional variation of NAA changes in AD was limited. Furthermore, most (but not all[15–17]) MRS studies of AD did not coanalyze metabolite data with quantitative MRI results. We described a multislice MRS imaging (MRSI) method for sampling the proton metabolite signal simultaneously from different regions in the brain, including surface cortex.[18] Based on coanalysis of MRSI with tissue segmented MRI data, we determined absolute metabolite signal intensities in normally aged brains, separately for GM, white matter (WM), and white matter lesions (WML) of the frontal and parietal lobes, and found age-related metabolite changes in addition to regional and tissue-dependent variations.

We first sought to determine the effects of AD on concentrations of NAA, Cr, and Cho in GM, WM, and WML in the frontal and parietal lobes of the brain by comparison with normal aging. Because histologic studies suggest that AD pathology impacts the parietal cortex earlier than the frontal cortex,[19] we tested the hypothesis that NAA differences between AD and normal aging are larger in parietal lobe GM than in frontal lobe GM and in WM.

In a previous MRI/MRSI study,[15] we found reduced NAA concentrations in the hippocampus of patients with AD compared with CN subjects, in addition to lower hippocampal volumes in AD. Furthermore, we showed that MRSI and MRI changes together improved discrimination between patients with AD and CN subjects relative to discriminations based on MRI alone. However, a shortfall of this earlier study was that NAA concentrations from other brain regions were not available to compare with changes in the hippocampus. In this study, MRSI data from the hippocampus and from frontal and parietal lobes were acquired in the same scan session, and coanalysis of MRSI with MRI data was expanded to account for variations in coverage of hippocampal tissue by MRSI. Therefore, we compared NAA of hippocampus and cortex in AD and CN. Because pathologic findings imply that AD initially involves the limbic structures, including the hippocampus, and eventually extends into the neo-cortex,[20] we tested the hypothesis that the most prominent NAA reductions in AD occur in the medial temporal lobe, including hippocampus.

We then assessed the extent to which NAA measurements by MRSI in combination with brain volume changes measured by MRI improve discrimination of patients with AD from CN subjects. In addition, we explored whether metabolite concentrations of WML would be different between AD and normal aging and whether Cho levels would be increased in AD.

Methods

Subjects

Fifty-six patients (mean age: 75.6 ± 8.0 years, 32 women) with a clinical diagnosis of AD according to the National Institute of Neurological and Communicative Disorders and Stroke-Alzheimer's Disease and Related Disorders Association (NINCDS-ADRDA) criteria[21] were recruited from the Goldman Institute on Aging and the Memory and Aging Clinic of the University of California at San Francisco (UCSF) and the Alzheimer Center of the University of California at Davis (UCD), and 54 CN subjects (mean age: 74.3 ± 8.1 years, 27 women) were recruited from the community and received standard neurologic examinations at the same centers. Patients with AD had Mini-Mental State Examination[22] (MMSE) scores between 16 and 26 out of 30. CN subjects had cognitive test scores within the normal, age-adjusted range

and no clinical history of alcoholism, psychiatric illness, epilepsy, hypertension, diabetes, major heart disease, or head trauma. Furthermore, a neuroradiologist evaluated the MRI data of all subjects, especially for presence of vascular pathology. Subjects were enrolled in this study if they had no lacunes and no other major vascular pathologies, except WML or atrophy. The committees of human research at UCSF and UCD and at the San Francisco Veterans Affairs Medical Center approved the study, and informed consent was obtained from each subject or his/her legal guardian before participation.

MRI and ^{1}H MRSI acquisition

MRI and ^{1}H MRSI data were obtained in one session on a 1.5 T Siemens Vision System (Siemens, Iselin, NJ), using a standard quadrature head coil. A vacuum-molded head holder (Vac-Pac, Olympic Medical, Seattle, WA) was used to restrict head movements. Structural MRI data included oblique axial double spin echo (DSE) images with repetition time/echo time 1/echo time 2 (TR/TE1/TE2) = 2500/20/80 milliseconds timing, 1.0 x 1.4 mm^2 inplane resolution, and 3-mm-thick sections with no section gap, oriented along the optic nerve as seen from a sagittal scout MR image, and covering the entire brain from the inferior cerebellum to the vertex. In addition to DSE, volumetric magnetization-prepared rapid gradient echo (MPRAGE) images were acquired with TR/TE/initial time (TI) = 10/7/300 milliseconds timing, 15° flip angle, 1.0 × 1.0 mm^2 inplane resolution, and 1.4-mm-thick coronal partitions, oriented orthogonal to the image planes of DSE. Proton density and T2-weighted images from DSE and T1-weighted images from MPRAGE were used together for tissue segmentation, and T1-weighted images from MPRAGE were used for manual editing of the hippocampus.

A point-resolved spectroscopy (PRESS) ^{1}H MRSI[23] sequence was used to acquire water suppressed ^{1}H MR spectra simultaneously from the left and right hippocampal region, as reported previously.[15] Timing was TR/TE = 1800/135 milliseconds and inplane resolution was 8.5 × 8.5 mm^2 with a 15-mm-thick section, aligned approximately along the long axis of the hippocampus, yielding a nominal voxel size of approximately 1.1 mL. Adjustment of Bo-field homogeneity (shimming) across the hippocampal region was performed manually. PRESS was used for acquiring metabolite spectra in the hippocampal region, because shimming had to be locally optimized and particularly strong lipid signals from orbital fat had to be removed, which could not be accomplished effectively by multislice MRSI. Multislice MRSI was used for sampling seamlessly large regions in the cortex, which is difficult to accomplish with volume selection by PRESS. Immediately after PRESS MRSI, Bo-field homogeneity was restored across the brain using an automated shimming routine and water-suppressed ^{1}H MR spectra were acquired from 2 axially oblique 15-mm-thick sections of the frontal and parietal brain using a multislice ^{1}H MRSI sequence with TR/TE = 1800/135 milliseconds timing. MRSI slices were parallel to the DSE image planes with the lowest slice positioned immediately below the superior aspect of the corpus callosum and the second slice 22 mm cephalad. This configuration covered large areas of the left and right frontal and parietal lobes with little inclusion of the occipital and temporal lobes and subcortical regions. k-Space sampling was accomplished with 36 × 36 circularly bounded encoding steps across a 280 × 280 mm^2 field of view, yielding a nominal MRSI voxel size of approximately 0.9 mL. Lipid signals were reduced using slice selective inversion recovery (TI = 170 milliseconds). Together, structural MRI, PRESS MRSI, and multislice ^{1}H MRSI, including shimming and adjustments, required approximately 90 minutes of acquisition time.

MRI volume measurements

Volumes of the left and right hippocampus were measured by manually drawing the boundaries of this structure on the coronal T1-weighted MR images, as reported peviously.[24] Tissue segmentation of MRI data into GM, WM, and CSF was achieved automatically with software developed in-house.[2] Additional operator-assisted segmentation classified further GM into

cortical GM and subcortical GM, WM into normal WM and WML, and CSF into sulcal and ventricular CSF. Furthermore, the interhemispheric fissure and the central sulcus were marked on MR images to determine the boundaries between the right and left cerebral hemispheres, and frontal and parietal lobes for coanalysis with MRSI. Finally, the masks of the left and right hippocampus from manual tracing also were incorporated into the segmentation data. Segmentation results were normalized to total intracranial volume to account for variations in head size among subjects. The raters were blinded to all clinical information and consistency of ratings (expressed as a coefficient of variation) was approximately 1.0% for hippocampus and better than 2% for tissue segmentation.

Spectral processing and MRI-MRSI coanalysis

PRESS ^{1}H MRSI data were zero-padded to 32 × 32 points in the spatial domain and were mildly filtered, resulting in an effective voxel size of about 1.6 mL. Along the spectral domain, data was zero-padded to 1024 points and peak areas of NAA, Cr, and Cho were estimated using fully automated spectral fitting software developed in-house.[25] Quality control was accomplished by rejecting spectra with more than 12-Hz line width or with residual sum squares of the fits in the upper 95th percentile. Typically, fewer than 10% of the spectra were rejected, predominantly from the prefrontal lobe because of problems with magnetic field inhomogeneity. The amounts of GM, WM, CSF, and left and right hippocampal tissue in each MRSI voxel were estimated using information from the segmented MRI data. This was accomplished first by aligning the segmented MRI with the MRSI data, assuming that there was no head movement between MRI and MRSI scans, and second by blurring the segmented MRI data to the spatial resolution of MRSI with consideration of chemical shift displacement effects. MRSI voxels in right and left hippocampus were automatically selected. First, the metabolite image was searched for the MRSI voxel with maximum amount of hippocampal tissue, followed by an evaluation of spectral quality. If spectral quality of this voxel was too poor, the voxel with the second largest amount of hippocampal tissue was selected, and so on until criteria for spectral quality were met. To obtain metabolite concentrations (in arbitrary units), the metabolite intensities were corrected for amounts of CSF in the MRSI voxels and normalized to the median ventricular CSF intensity on proton density MR images.

Spectral processing of multislice ^{1}H MRSI data was similar to PRESS ^{1}H MRSI. First, the data were zero-padded to 64 × 64 points with no additional filtering in the spatial domain and to 1024 points in the spectral domain. Reduction of spurious resonances from extracranial lipids was accomplished by selective k-space extrapolation.[26] The peak areas of NAA, Cr, and Cho were estimated using the same spectral fitting software package, criteria for quality control, and corrections for receiver gain and CSF intensity as described before for PRESS MRSI. The next goal was to separate contributions from GM, WM, and WML to the metabolite signal and to correct for CSF content in MRSI voxels for obtaining metabolite concentrations. These separate contributions were estimated by regressing metabolite intensity variations against variations in tissue composition across MRSI voxels, which was estimated from tissue segmented MRI data, coregistered to MRSI, and described previously.[18] The regression coefficients represent metabolite intensities per volume GM or WM tissue, which is synonymous with concentration (in arbitrary units) in this context and are the values reported here. However, because T1 and T2 were not measured and intensity was not calibrated, metabolite concentrations from the regressions cannot be compared directly with absolute concentrations in units of mmol/L. Estimations of [NAA], [Cr], and [Cho] from regressions were obtained separately for GM and WM of the left and right frontal and parietal lobes, and for WML. Spurious contributions to the metabolite signal from other tissue types and regions, such as subcortical GM or occipital lobe, were accounted for by screening out MRSI voxels from these regions.

Statistical analysis

Regional differences in metabolite concentrations between AD and CN subjects were tested using multivariate analysis of variance (MANOVA) and accounting for age. Metabolite concentrations were dependent variables and regions, diagnosis, and age were independent variables. To reduce the probability of finding by chance significant metabolite variations in any region, the level of significance for MANOVA was increased to $\alpha = 0.05/9 = 0.006$, using Bonferroni corrections for multiple comparisons (9 independent tests for [NAA], [Cho], and [Cr] in GM, WM, and hippocampus; tests for WML were not considered as multiple comparisons, because large WM lesions were found only in a small group of subjects). Statistical tests other than MANOVA were performed with $\alpha = 0.05$. ANOVA was used to test differences between groups in WML. To compare PRESS and multislice MRSI data without needing to account for experimental differences between the two techniques, metabolite concentrations were transformed into z-scores, according to $z[Met]_k^j = ([Met]_k^j - mean[Met]_k^{CN}) / stdev[Met]_k^{CN}$. Here, $z[Met]_k^j$ represents a z-score of a metabolite in brain region k (= hippocampus, frontal or parietal left or right GM or WM) of patient j, $[Met]_k^j$ is the concentration of the corresponding metabolite, and $mean[Met]_k^j$ and $stdev[Met]_k^j$ are the metabolite mean and SD in region k in the CN group. Pearson product moment coefficients were used to evaluate correlations between measures. Logistic regression was performed to determine the contributions from MRI and MRSI to the classification of AD and CN subjects. Furthermore, receiver operator characteristics (ROC) analysis was performed to provide a means of comparing MRI and MRSI classifiers in terms of sensitivity and specificity. Unless noted otherwise, all data are listed as mean ± SD.

Results

Table 1 lists demographic data of the subjects, separately for those who completed only PRESS MRSI and those who also completed multislice MRSI. AD and CN were comparable in age ($p > 0.4$ by Student's *t*-test) without a difference between PRESS or multislice MRSI groups ($p > 0.5$). Men and women were comparably represented in the AD and CN group ($p = 0.5$ for PRESS and $p = 0.6$ for multislice MRSI, both by χ^2 test). As expected, patients with AD had lower MMSE scores than CN subjects ($p < 0.0001$ by Student's *t*-test).

Figure 1 shows representative metabolite images of the medial temporal lobe (obtained with PRESS MRSI) and the frontal and parietal lobes (obtained with multislice MRSI) from a 58-year-old man with AD and a 59-year-old cognitively normal man. Also shown in figure 1 are representative ^{1}H MR spectra from selected regions of hippocampus and frontal and parietal lobe GM in the patient with and CN subject. ^{1}H MR spectra from the patient with AD depict lower intensities for NAA relative to Cho and Cr compared with ^{1}H MR spectra from the healthy subject.

Table 2 lists [NAA] concentrations in the medial temporal lobe of AD and CN. Also listed is the amount of hippocampal tissue enclosed in MRSI voxels from this region, expressed as percent of total brain tissue within voxels. [NAA] was less in AD by 21% in both the left [$F = 27.1$, $df = 1,106$, $p < 0.0001$] and the right [$F = 24.3$, $df = 1,106$, $p < 0.0001$] sides compared with CN, even after accounting for variations in the amount of hippocampal tissue in MRSI voxels. Effects of hemisphere or hemisphere-by-group interactions on [NAA] changes were not significant. Differences of both [Cho] and [Cr] (not listed) between AD and CN were not significant in the hippocampal region at the adjusted α level. MRSI voxels contained on average 18% to 19% hippocampal tissue in patients with AD and 21% to 26% in CN subjects without difference between the groups ($p > 0.2$, by Student's *t*-test). Sex had no effect on metabolite differences in this region ($p > 0.2$, by Student's *t*-test).

Table 2 also lists [NAA] of GM and WM in the frontal and parietal lobes of AD and CN. The most prominent differences between AD and CN were 18% lower [NAA] in left parietal GM [F = 10.5, *df* = 1,78, *p* = 0.001] and 13% lower [NAA] in right parietal GM [F = 9.6, *df* = 1,78, *p* = 0.003] of AD without left/right differences. In contrast to the parietal lobe, there were no [NAA] differences of frontal lobe GM between AD and CN at the adjusted α level (left [F = 1.5, *df* = 1,78, *p* = 0.17], right [F = 4.0, *df* = 1,78, *p* = 0.04]). [NAA] differences between AD and CN in both frontal and parietal lobe WM also were not significant. [Cho] and [Cr] differences (not listed) between AD and CN in both GM and WM were not significant.

Table 3 lists [NAA], [Cho], and [Cr] of WML and WM in 17 patients with AD and 11 CN subjects, who had lesions that were large relative to the resolution of MRSI. [NAA] differences of WML between the groups were not significant. However, [NAA] of WML was less than [NAA] of WM by approximately 15% [F = 9.2, *df* = 1,27, *p* = 0.005] in both groups. Both [Cho] and [Cr] of WML were not different between patients with AD and CN subjects, and [Cho] and [Cr] did not differ significantly between WML and WM.

To test whether [NAA] changes in the medial temporal lobe were different from changes in the frontal and parietal lobes, we transformed the NAA data into z-scores. [NAA] z-scores of patients with AD in different brain regions are shown in figure 2. Overall, regional variations of [NAA] z-scores in AD were significant [F = 9.1, *df* = 3,155, *p* < 0.0001, by ANOVA]. Post hoc Scheffe tests showed that [NAA] reductions in the medial temporal lobe of AD were greater than changes in both frontal lobe GM [F = 6.2, *df* = 1,84, *p* = 0.01] and WM [F = 30.4, *df* = 1,84, *p* < 0.0001], but were similar to changes in parietal lobe GM [F = 0.1, *df* = 1,84, *p* > 0.7]. [NAA] changes of parietal GM in AD also were larger than changes of frontal lobe GM [F = 3.1, *df* = 1,70, *p* = 0.05] and WM [F = 14.5, *df* = 1,70, *p* < 0.0005]. We also explored whether [NAA] reductions in the medial temporal lobe and parietal lobe GM were correlated in patients with AD, but found no correlation (*r* = 0.22, *p* > 0.1). Furthermore, we found a trend for correlations between MMSE scores of the patients and [NAA] reductions in the medial temporal lobe (*r* = 0.25, *p* = 0.06) and parietal GM (*r* = 0.23, *p* = 0.08).

Table 4 lists results from tissue-segmented MRI data of patients with AD and CN subjects. This shows that patients with AD compared with CN subjects had smaller volumes of hippocampus (*p* < 0.0001, by Student's *t*-test), GM (*p* < 0.001), and WM (*p* < 00001), and larger volumes of ventricular CSF (*p* < 0.0001) and WML (*p* < 0.01). However, these volume changes did not correlate with MMSE scores (all *p* > 0.3).

Finally, we tested the extent to which [NAA] measurements by MRSI combined with volume measurements by MRI improve discrimination between AD and CN. Table 5 lists sensitivity, specificity, and overall correct classification of AD and CN for those combinations of MRSI and MRI measures that made significant contributions to the classification. Also listed are the areas under the curve from a ROC analysis. Prediction of group membership by hippocampal volume alone was significant (*p* > 0.0001), yielding a ROC area under the curve of 0.89. Adding [NAA] of medial temporal lobe improved (*p* = 0.004) classification and increased significantly the area under the curve to 0.93. Cortical GM volume from MRI made another contribution to classification (*p* = 0.0001) and also significantly increased the area under the curve to 0.95. Additional contributions from [NAA] and volume measures were not significant.

Discussion

The major findings of this study were: first, [NAA] reductions in AD occurred primarily in medial temporal lobe, including hippocampus and parietal lobe GM (not WM), and these reductions were of similar magnitude. Second, [NAA] reductions in the frontal lobe of AD were significantly less than in medial temporal and parietal lobe. Third, [NAA] and volume

changes together provided better discrimination between patients and control subjects than volume changes alone, similar to the results from our previous study,[15] which focused on a different group of patients with AD and CN subjects. Taken together, these results emphasize the additional diagnostic information obtained by ^{1}H MRSI.

The finding of substantial [NAA] reductions in GM of patients with AD compared with control subjects and virtually no differences in WM is consistent with another MRSI study[16] that used a similar method for separation of GM and WM contributions to metabolite changes in AD, but did not measure separately in the frontal and parietal lobes. [NAA] reductions in GM with little or no change in WM also are consistent with a MRS study[27] of postmortem AD brains and with histopathologic findings that AD is predominantly a disease of the cerebral cortex.[28] In addition to GM and WM differences, we also found larger [NAA] reductions in parietal than frontal lobe GM, agreeing with PET studies of AD that revealed severe deficits in cerebral blood flow and glucose metabolism, especially in parietal and temporal lobe region.[29] In contrast to this study, another multislice MRSI[30] reported reduced NAA ratios (not absolute NAA concentrations and not corrected for partial volume effects) in the frontal cortex of AD in addition to changes in parietal and temporal lobes. One single voxel MRS study also reported reduced NAA ratios in frontal brain regions of AD.[14] A possible explanation for the divergent findings is that this study excluded patients with AD with subcortical lacunar infarcts, which can be partly responsible for [NAA] reductions in cortical regions,[31] whereas other studies did not screen for subcortical infarctions. We also found [NAA] reductions in medial temporal lobe in AD, agreeing with several earlier MRS studies.[15,32,33] Reduced [NAA] may indicate disproportionately greater loss of neurons than glia or it could indicate impaired neuronal metabolism without neuron loss.

In contrast to our first MRSI report of AD[11] and quantitative MRSI studies by others,[16,34,35] we found no increase of [Cho] in AD. Other MRS studies[36,37] also found no [Cho] changes in AD and one study reported decreased Cho ratios.[30] Limited accuracy in measuring [Cho] could explain some of the divergent findings of Cho changes in AD, especially in cortical regions with low signal intensities. Furthermore, some MRSI studies found marked [Cho] changes predominantly in subcortical GM of AD,[30] which were screened out for this analysis.

We found no significant metabolite differences between patients with AD and CN subjects in WML. Compared with normal WM, however, [NAA] of WML was significantly reduced in both AD and CN, consistent with an earlier report from this laboratory.[38] Inconsistent with previous findings, however, we found no increase of [Cho] in WML.[38]

Another result was that the combination of MRI and MRSI measures provided an improved classification between AD and control subjects compared with either measure alone. However, an overlap between the groups remained when [NAA] and volume were used individually or together. Therefore, this will not lead to a diagnosis of the individual patient unless more information is incorporated, such as MRS measurements of *myo*-inositol.[35] Furthermore, clinically more important than separating AD from normal aging is a differentiation of AD from other types of dementias.

This study has several limitations. First, measurements for obtaining relaxation values of metabolites could not be performed because of prohibitively long acquisition times, although T1 and T2 for AD have been previously determined for two brain locations.[39] Therefore, corrections for T2 and T1 relaxations (especially important because of use of slice-selective inversion recovery) were not applied, and absolute metabolite concentrations in units of mole per tissue volume were not determined. Second, because we applied a medium spin-echo time acquisition (TE = 135 milliseconds), metabolites with shorter T2 relaxation times, such as *myo*-inositol, could not be observed. It has been reported previously that *myo*-inositol is

increased in AD and that the combined use of *myo*-inositol and NAA increases diagnostic sensitivity.[40] Third, frontal and parietal GM was not differentiated further into GM of the sensory and the motor cortex. Provided that primary sensory and motor cortex are among the last cortical regions to be affected in the AD process,[19] [NAA] change in AD therefore could be biased for varying contributions from these regions. Finally, spatial resolution of tissue-segmented MRI data was compromised, because the segmentation algorithm was based on both T1-weighted MR images of relative high resolution and T2-weighted MR images of lower resolution than the T1-weighted images. It is possible that different results would be obtained if segmentation were performed with the better resolution of T1-weighted MR data. However, T1-weighted MRI is insensitive to the effects of vascular disease, such as WML, which is an important confound in studies of aging and dementia.

Acknowledgements

The authors thank Mr. Sean Steinman and Ms. Marybeth Kedzior for help with data acquisition and processing.

References

1. Jack CRJ, Petersen RC, O'Brien PC, Tangalos EG. MR-based hippocampal volumetry in the diagnosis of Alzheimer's disease. Neurology 1992;42:183–188. [PubMed: 1734300]
2. Tanabe JL, Amend D, Schuff N, et al. Tissue segmentation of the brain in Alzheimer disease. AJNR Am J Neuroradiol 1997;18:115–123. [PubMed: 9010529]
3. Rombouts SA, Barkhof F, Witter MP, Scheltens P. Unbiased whole-brain analysis of gray matter loss in Alzheimer's disease. Neurosci Lett 2000;285:231–233. [PubMed: 10806328]
4. Jernigan TL, Archibald SL, Berhow MT, Sowell ER, Foster DS, Hesselink JR. Cerebral structure on MRI. Part I: localization of age-related changes. Biol Psychiatry 1991;29:55–67. [PubMed: 2001446]
5. Pfefferbaum A, Mathalon DH, Sullivan EV, Rawles JM, Zipur-sky RB, Lim KO. A quantitative magnetic resonance imaging study of changes in brain morphology from infancy to late adulthood. Arch Neurol 1994;51:874 –887. [PubMed: 8080387]
6. Flood DG, Coleman PD. Hippocampal plasticity in normal aging and decreased plasticity in Alzheimer's disease. Prog Brain Res 1990;83:435–443. [PubMed: 2203107]
7. Simic G, Kostovic I, Winblad B, Bogdanovic N. Volume and number of neurons of the human hippocampal formation in normal aging and Alzheimer's disease. J Comp Neurol 1997;379:482–494. [PubMed: 9067838]
8. Birken DL, Oldendorf WH. N-acetyl-L-aspartic acid: a literature review of a compound prominent in 1H-NMR spectroscopic studies of brain. Neurosci Biobehav Rev 1989;13:23–31. [PubMed: 2671831]
9. Lu D, Margouleff C, Rubin E, et al. Temporal lobe epilepsy: correlation of proton magnetic resonance spectroscopy and 18F-fluorodeoxyglucose positron emission tomography. Magn Reson Med 1997;37:18 –23. [PubMed: 8978628]
10. Clark JB. N-acetyl aspartate: a marker for neuronal loss or mitochondrial dysfunction. Dev Neurosci 1998;20:271–276. [PubMed: 9778562]
11. Meyerhoff DJ, MacKay S, Constans JM, et al. Axonal injury and membrane alterations in Alzheimer's disease suggested by in vivo proton magnetic resonance spectroscopic imaging. Ann Neurol 1994;36:40 –47. [PubMed: 8024260]
12. Ross BD, Bluml S, Cowan R, Danielsen E, Farrow N, Tan J. In vivo MR spectroscopy of human dementia. Neuroimaging Clin N Am 1998;8:809 –822. [PubMed: 9769343]
13. Shonk TK, Moats RA, Gifford P, et al. Probable Alzheimer disease: diagnosis with proton MR spectroscopy. Radiology 1995;195:65–72. [PubMed: 7892497]
14. Parnetti L, Lowenthal DT, Presciutti O, et al. 1H-MRS, MRI-based hippocampal volumetry, and 99mTc-HMPAO-SPECT in normal aging, age-associated memory impairment, and probable Alzheimer's disease [see comments]. J Am Geriatr Soc 1996;44:133–138. [PubMed: 8576501]
15. Schuff N, Amend D, Ezekiel F, et al. Changes of hippocampal n-acetyl aspartate and volume in Alzheimer's disease: a proton MR spectroscopic imaging and MRI study. Neurology 1997;49:1513–1521. [PubMed: 9409338]

16. Pfefferbaum A, Adalsteinsson E, Spielman D, Sullivan EV, Lim KO. In vivo brain concentrations of N-acetyl compounds, creatine, and choline in Alzheimer disease. Arch General Psychiatry 1999;56:185–192.
17. MacKay S, Ezekiel F, Di Sciafani V, et al. Alzheimer disease and subcortical ischemic vascular dementia: evaluation by combining MR imaging segmentation and H-1 MR spectroscopic imaging. Radiology 1996;198:537–545. [PubMed: 8596863]
18. Schuff N, Ezekiel F, Gamst A, et al. Region and tissue differences of metabolites in normally aged brain using 1H magnetic resonance spectroscopic imaging. Magn Reson Med 2001;45:899 –907. [PubMed: 11323817]
19. Braak H, Braak E. Staging of Alzheimer's disease-related neurofibrillary changes. Neuobiol Aging 1995;16:271–278.
20. Braak H, Braak E, Bohl J. Staging of Alzheimer-related cortical destruction. Eur Neurol 1993;33:403–408. [PubMed: 8307060]
21. Tierney MC, Fisher RH, Lewis AJ, et al. The NINCDS-ADRDA Work Group criteria for the clinical diagnosis of probable Alzheimer's disease: a clinicopathologic study of 57 cases [see comments]. Neurology 1988;38:359 –364. [PubMed: 3347338]
22. Folstein MF, Folstein SE, McHugh PR. 'Mini-mental state'. A practical method for grading the cognitive state of patients for the clinician. J Psychiatr Res 1975;12:189 –198. [PubMed: 1202204]
23. Bottomley PA. Spatial localization in NMR spectroscopy in vivo. Ann NY Acad Sci 1987;508:333–348. [PubMed: 3326459]
24. Du A, Schuff N, Amend D, et al. MRI of entorhinal cortex and Hippocampus in Mild Cognitive Impairment and Alzheimer's Disease. Journal of Neurology, Neurosurgery, and Psychiatry 2001;71:441–447.
25. Soher BJ, Young K, Govindaraju V, Maudsley AA. Automated spectral analysis III: application to in vivo proton MR spectroscopy and spectroscopic imaging. Magn Reson Med 1998;40:822–831. [PubMed: 9840826]
26. Haupt CI, Schuff N, Weiner MW, Maudsley AA. Removal of lipid artifacts in 1H spectroscopic imaging by data extrapolation. Magn Reson Med 1996;35:678 –687. [PubMed: 8722819]
27. Kwo-On-Yuen P, Newmark RD, Budinger TF, Kaye JA, Ball MJ, Jagust WJ. Brain N-acetyl-L-aspartic acid in Alzheimer's disease: a proton magnetic resonance spectroscopy study. Brain Res 1994;667:167–174. [PubMed: 7697354]
28. Hyman BT, Gomez-Isla T. Alzheimer's disease is a laminar, regional, and neural system specific disease, not a global brain disease. Neurobiol Aging 1994;15:353–354. [PubMed: 7936060]
29. Jagust WJ. Functional imaging in dementia: an overview. J Clin Psychiatry 1994;55(suppl):5–11. [PubMed: 7989292]
30. Tedeschi G, Bertolino A, Lundbom N, et al. Cortical and subcortical chemical pathology in Alzheimer's disease as assessed by multislice proton magnetic resonance spectroscopic imaging. Neurology 1996;47:696 –704. [PubMed: 8797467]
31. Capizzano AA, Schuff N, Amend DL, et al. Subcortical ischemic vascular dementia: assessment with quantitative MR imaging and 1H MR spectroscopy. AJNR Am J Neuroradiol 2000;21:621–630. [PubMed: 10782769]
32. Jessen F, Block W, Traber F, et al. Proton MR spectroscopy detects a relative decrease of N-acetylaspartate in the medial temporal lobe of patients with AD. Neurology 2000;55:684 –688. [PubMed: 10980734]
33. Mohanakrishnan P, Fowler AH, Vonsattel JP, et al. An in vitro 1H nuclear magnetic resonance study of the temporoparietal cortex of Alzheimer brains. Exp Brain Res 1995;102:503–510. [PubMed: 7737396]
34. Lazeyras F, Charles HC, Tupler LA, Erickson R, Boyko OB, Krishnan KR. Metabolic brain mapping in Alzheimer's disease using proton magnetic resonance spectroscopy. Psychiatry Res 1998;82:95–106. [PubMed: 9754452]
35. Kantarci K, Jack CJ, Xu YC, et al. Regional metabolic patterns in mild cognitive impairment and Alzheimer's disease: a 1H MRS study. Neurology 2000;55:210 –217. [PubMed: 10908893]

36. Rose SE, de Zubicaray GI, Wang D, et al. A 1H MRS study of probable Alzheimer's disease and normal aging: implications for longitudinal monitoring of dementia progression. Magn Reson Imaging 1999;17:291–299. [PubMed: 10215485]

37. Stoppe G, Bruhn H, Pouwels PJ, Hanicke W, Frahm J. Alzheimer disease: absolute quantification of cerebral metabolites in vivo using localized proton magnetic resonance spectroscopy. Alzheimer Dis Assoc Disord 2000;14:112–119. [PubMed: 10850750]

38. Constans J-M, Meyerhoff DJ, Gerson J, et al. H-1 MR spectroscopic imaging of white matter signal hyperintensities: Alzheimer disease and ischemic vascular dementia. Radiology 1995;197:517–523. [PubMed: 7480705]

39. Moats RA, Ernst T, Shonk TK, Ross BD. Abnormal cerebral metabolite concentrations in patients with probable Alzheimer disease. Magn Reson Med 1994;32:110 –115. [PubMed: 8084225]

40. Miller BL, Moats RA, Shonk T, Ernst T, Woolley S, Ross BD. Alzheimer disease: depiction of increased cerebral myoinositol with proton MR spectroscopy. Radiology 1993;187:433–437. [PubMed: 8475286]

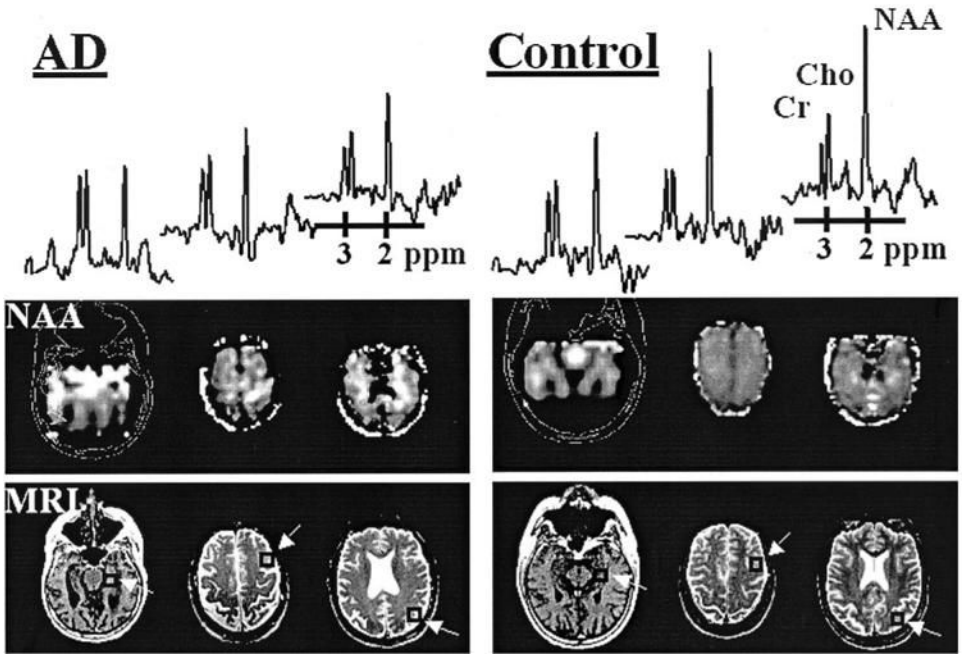

Figure 1.

Proton MR (^{1}H MR) spectra and *N*-acetylaspartate (NAA) images from a 58-year-old patient with AD and a 59-year-old cognitively normal control subject. The ^{1}H MR spectra (from left to right) were selected from the hippocampus, frontal lobe, and parietal lobe (arrows point to regions of interest indicated by squares). The spectra differ between the two subjects in vertical scale and therefore cannot be compared directly. Also shown are the corresponding structural MRI data for anatomic reference of the low-resolution NAA images.

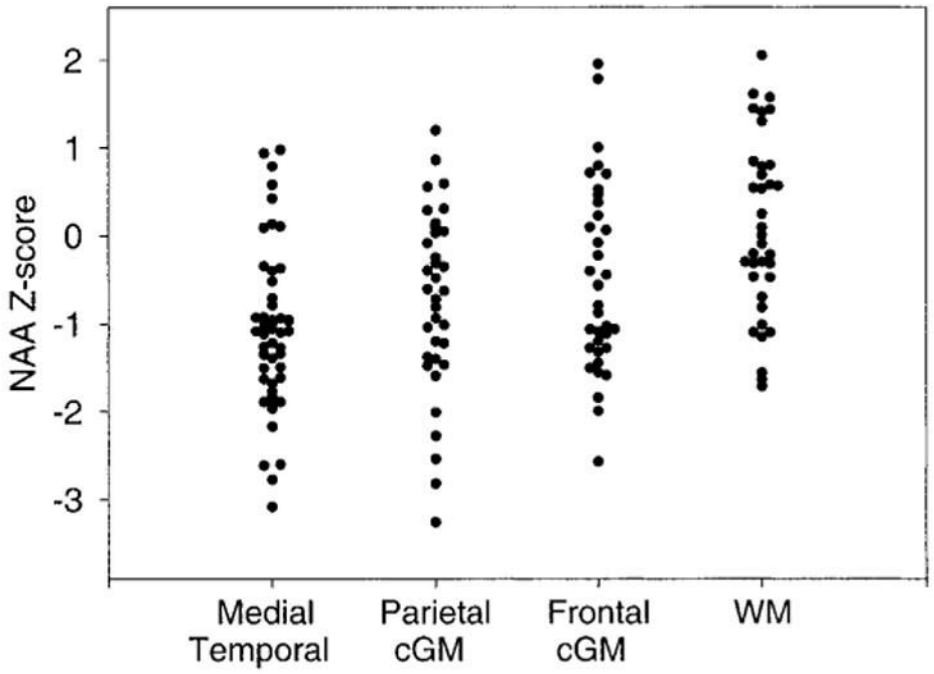

Figure 2.
Reduction of *N*-acetylaspartate (NAA) concentration in different brain regions in patients with AD. Values are in Z-scores, relative to a mean NAA concentration for cognitively normal subjects of zero. cGM = cortical gray matter; WM = white matter.

Table 1

Demographics

Parameters	PRESS		PRESS and multislice	
	AD	Control	AD	Control
Subjects, n	56	54	41	40
Female/male	32/24	27/27	25/16	22/18
Mean age, y	75.6 ± 8.0	74.3 ± 8.1	74.6 ± 7.1	74.2 ± 8.4
Age range, y	56–87	48–88	58–87	48–88
MMSE[22]	19.0 ± 6.7	29.1 ± 0.8	19.0 ± 6.8	29.1 ± 0.8

Subjects listed under PRESS and multislice MRSI belong to the 56 patients with AD and 54 control subjects under PRESS.

PRESS = point-resolved spectroscopy; MMSE = Mini-Mental State Examination.

Table 2

NAA concentration in medial temporal lobe, including hippocampus and in frontal and parietal lobe gray matter and white matter

Brain region	Side	Tissue	AD	Control	AD-control*
Medial temporal†	Left	Gray + white	1.81 ± 0.44	2.29 ± 0.50	−21//
	Right	Gray + white	1.80 ± 0.47	2.29 ± 0.51	−21//
Frontal‡	Left	Gray	0.95 ± 0.21	1.02 ± 0.16	−7
	Right	Gray	0.92 ± 0.20	1.03 ± 0.19	−11
	Left	White	1.12 ± 0.25	1.13 ± 0.20	−1
	Right	White	1.11 ± 0.21	1.11 ± 0.20	0
Parietal‡	Left	Gray	0.83 ± 0.26	1.01 ± 0.19	−18¶
	Right	Gray	0.90 ± 0.20	1.03 ± 0.21	−13¶
	Left	White	1.21 ± 0.22	1.19 ± 0.19	−2
	Right	White	1.17 ± 0.22	1.15 ± 0.17	−2
HP tissue [%]§	Left		18.1 ± 7.7	21.6 ± 8.0	−18
	Right		19.3 ± 6.6	26.5 ± 8.4	−26

N-acetylaspartate (NAA) concentration in arbitrary units.

*Percent change in patients with AD compared with cognitively normal subjects.

†From 56 patients with AD and 54 control subjects.

‡From 41 patients with AD and 40 control subjects.

§Percent hippocampal (HP) tissue of total tissue content in MRS imaging voxels from medial temporal lobe.

//$p < 0.001$.

¶$p < 0.003$.

Table 3

Metabolite concentrations in white matter lesions and normal white matter

Metabolite*	Tissue	AD	Control	AD-control†
[NAA]	WML	1.01 ± 0.54	0.99 ± 0.43	+2
	WM	1.16 ± 0.22	1.19 ± 0.24	−3
[Cho]	WML	0.55 ± 0.32	0.51 ± 0.38	+8
	WM	0.42 ± 0.11	0.44 ± 0.07	−4
[Cr]	WML	0.48 ± 0.19	0.45 ± 0.29	+7
	WM	0.45 ± 0.10	0.47 ± 0.09	−4

*Concentration in arbitrary units.

†Percent change in 41 patients with AD compared with 40 cognitively normal subjects.

WML = white matter lesion; WM = white matter (normal).

Table 4

Brain volume changes

Volumes*	AD	Control	AD-control†	*p* Value
Hippocampus, mm^3	1886 ± 484	2669 ± 364	−29	<0.0001
Cortical gray matter, cm^3	453 ± 37	508 ± 32	−11	<0.0001
White matter, cm^3	437 ± 37	465 ± 32	−6	0.0003
Ventricular space, cm^2	72 ± 29	44 ± 14	62	<0.0001
White matter lesions, cm^2	13 ± 14	7 ± 9	86	>0.01

*All volumes normalized to total intracranial volume.

†Percent change in 56 patients with AD compared with 54 cognitively normal subjects.

Table 5

Classification of patients with AD and cognitively normal subjects

Measures	Sensitivity*	Specificity*	Overall*	ROC†	*p* Value‡
Hippocampal volume	0.82	0.81	0.81	0.89	<0.0001
+ [NAA]§	0.84	0.83	0.83	0.93	0.004
+ Gray matter volume	0.91	0.86	0.88	0.95	0.0001

*Using logistic regression analysis in 41 patients with AD and 40 control subjects.

†Receiver operator characteristic (ROC) area under the curve.

‡Analysis by logistic regression.

§In medial temporal lobe.